

COMMUNICATION

Supporting Information

**Picoplatin binding to proteins: X-ray structures and mass spectrometry
data on the adducts with lysozyme and ribonuclease A**

Giarita Ferraro,^a Tereza Lyčková,^b Lara Massai,^c Pavel Starha,^b Luigi Messori^c and Antonello Merlino^{a*}

^a Department of Chemical Sciences, University of Naples Federico II, Complesso universitario di Monte Sant'Angelo, via Cinthia, 21, 80126, Naples, Italy. Email: antonello.merlino@unina.it

^b Department of Inorganic Chemistry, Faculty of Science, Palacký University Olomouc, 17. listopadu 12, 771 46 Olomouc, Czech Republic

^c Department of Chemistry "Ugo Schiff", University of Florence, via della Lastruccia, 3-13, 50019, Sesto Fiorentino, Florence, Italy

COMMUNICATION

Materials and Methods.	Pag. 3
Results	Pag. 5
Figure S1.	Pag. 6
Figure S2.	Pag. 7
Figure S3.	Pag. 8
Figure S4.	Pag. 9
Figure S5.	Pag. 10
Figure S6.	Pag. 11
Figure S7.	Pag. 12
Figure S8.	Pag. 13
Table S1.	Pag. 14
Table S2.	Pag. 15
References	Pag. 16

Materials and Methods

Materials

Picoplatin was synthetized as previously reported [1] and its composition and purity was checked by CHN analysis and ^1H NMR spectroscopy. CHN Anal. (for $\text{C}_6\text{H}_{10}\text{N}_2\text{Cl}_2\text{Pt}$): Calcd.: C, 19.16; H, 2.68; N, 7.45; Found: C, 19.24; H, 2.74; N, 7.16%. ^1H NMR ($\text{DMF}-d_7$): 9.02 (d, $J_{\text{HH}} = 5.3$ Hz, py), 7.87 (m, py), 7.55 (d, $J_{\text{HH}} = 8.3$ Hz, py), 7.33 (t, $J_{\text{HH}} = 6.6$ Hz, py), 4.43 (br, NH_3), 3.16 (s, CH_3) ppm. HEWL and RNase A were purchased from Sigma Chemical Co and used without further purification. All the other reagents were of analytical grade.

Stability studies of picoplatin

Appropriate amount of picoplatin (for 0.1 mM final concentration) was dissolved in 600 μL of $\text{DMSO}-d_6$, 600 μL of 10% $\text{DMSO}-d_6/90\%$ D_2O , 600 μL of 1% $\text{DMSO}-d_6/99\%$ D_2O , 600 μL of 10% $\text{DMSO}-d_6/90\%$ PBS in D_2O or 600 μL of 1% $\text{DMSO}-d_6/99\%$ PBS in D_2O . ^1H NMR spectra were recorded at various time points up to 24 h of standing at r.t. ^1H NMR spectrum of free α -picoline was recorded as well for comparative purposes in the same solvents.

Analogue ESI $^+$ mass spectrometry experiments were performed in non-deuterated solvents. In this case, 10 μL of the studied DMSO-containing samples were added to 300 μL of MeOH (LC grade) for the MS analysis.

General methods

Elemental analyses (C, H, N) were carried out by a Flash 2000 CHNS Elemental Analyser (Thermo Scientific). ^1H NMR spectra were recorded using Bruker and JEOL 400 MHz spectrometers and the spectra were calibrated against the residual signals of the used solvents. Mass spectrometry was performed on the MeOH solution using a LCQ Fleet Ion Trap spectrometer (Thermo Scientific; Qual Browser software, version 2.0.7) in the positive electrospray ionization mode (ESI $^+$).

ESI MS measurements

Sample preparation.

HEWL and RNase A 10^{-3} M stock solutions were prepared, dissolving the proteins in LC-MS grade water. Stock solution of picoplatin was prepared in DMSO to a final concentration of 3×10^{-2} M. To prepare solutions for experiments with proteins and platinum complexes, 100 μM solutions of the protein and picoplatin were prepared at a 1:3 protein-to-metal ratio by dilution with 20 mM ammonium acetate buffer (pH 6.8). The final DMSO concentration in the incubation solution was 1%. The mixtures were then incubated at 37 °C up to 24 h.

Electrospray Ionization Mass Spectrometry Analysis:

Final Dilutions. After the incubation time, all protein solutions were sampled and diluted to a final protein concentration of 5×10^{-7} M using ammonium acetate. 0.1% v/v of formic acid was added just before infusion in the mass spectrometer.

Instrumental Parameters. the ESI mass study was performed using a TripleTOF R 5600+ high-resolution mass spectrometer (Sciex, Framingham, MA, United States), equipped with a DuoSpray R interface operating with an ESI probe. Respective ESI MS spectra were acquired through direct infusion at a 7 $\mu\text{l}/\text{min}$ flow rate. The general ESI source parameters optimized for each protein analysis were as follows, *HEWL* positive polarity: ion spray voltage floating 5,500V, temperature 0, ion source Gas 1 (GS1) 40 L/min; ion source Gas 2 (GS2) 0; CUR 20 L/min, CE 10V; DP 100V, range 1200–3000 m/z. *RNase A*: positive

polarity, ionspray voltage floating 5500 V, temperature 0, ion source gas 1 (GS1) 40 L/min; ion source gas 2 (GS2) 0; curtain gas (CUR) 15 L/min, declustering potential (DP) 100 V, collision energy (CE) 10 V, range 1200–3000 m/z;

For acquisition, Analyst TF software 1.7.1 (Sciex) was used and deconvoluted spectra were obtained by using the Bio Tool Kit micro-application v.2.2 embedded in the PeakView™ software v.2.2 (Sciex).

Crystallization, X-ray diffraction data collection, structure solution and refinement

Crystals of HEWL and RNase A in the presence of picoplatin were obtained by soaking [2] experiments. Crystals of the metal-free HEWL were grown by hanging drop vapour diffusion method using a reservoir solution containing 20% ethylene glycol, 0.6 M sodium nitrate and 0.1 sodium acetate pH 4.5 ($[\text{protein}] = 13 \text{ mg mL}^{-1}$). Crystals of metal-free RNase A were grown by hanging drop vapour diffusion method using a reservoir solution containing 22% PEG4000, 0.1 M sodium citrate pH 5.1 ($[\text{protein}] = 20 \text{ mg mL}^{-1}$).

These crystals were soaked for 3 days with a solution containing 50% reservoir and 50% picoplatin dissolved in pure DMSO (final protein to metal molar ratio = 1:3) in the case of structure **A**, and in a solution of the reservoir saturated with picoplatin powder, in the case of structure **B**. In the case of RNase A, crystals were soaked with picoplatin powder (structure **D**) and then 30% DMSO was added to the solution containing RNase A crystals and picoplatin (structure **C**). X-ray diffraction data were then collected at XRD2 beamline of Elettra synchrotron in Trieste, Italy at 1.36 and 1.60 Å resolution for the best crystals of HEWL with picoplatin and at 1.76 and 1.99 Å resolution for the crystals of RNase A treated with the drug. Data were processed with AutoProc [3]. Data collection statistics are reported in Table S1. Results of the structural analysis carried out on the adduct with HEWL were confirmed by an additional crystal that diffracts X-ray at 1.52 Å resolution (data not shown). The structures were solved by molecular replacement using Phaser [4] and the coordinates of metal-free proteins from PDB codes 1JVT [5] and 193L [6] as starting models. Restrained refinement has been performed using Refmac5 [7]. Refinement statistics are reported in Table S1. Inspection of electron density maps and model building have been carried out using Coot [8].

Results

Stability studies in DMSO-containing solutions

The ^1H NMR results clearly proved that picoplatin began to transform after the dissolution in DMSO. Along with the characteristic ^1H NMR C6–H resonance of picoplatin ($\delta = 8.81$ ppm), new C6–H signals were detected as well (Figure S1). The dominant one ($\delta = 8.40$ ppm) can be unambiguously assigned to free α -picoline, which released from picoplatin in DMSO (Figure S1). The ratio of picoplatin and free α -picoline was *ca.* 1:4 after 24 h of standing at r.t. This is also supported by the detection of $-\text{CH}_3$ resonance of free α -picoline at 2.42 ppm (overlapped with the DMSO signal), together with the same signal of picoplatin ($\delta = 3.02$ ppm).

Since the samples for the crystallization with proteins contained 1% DMSO, we also studied the stability of picoplatin in various DMSO-containing mixtures of solvents with water or PBS in water (^1H NMR, ESI-MS). Interestingly, no release of α -picoline was observed by ^1H NMR in 10% DMSO- d_6 /90% D_2O (Figure S2) and in 1% DMSO- d_6 /99% D_2O (Figure S3). Even without the release of the pic ligand, picoplatin is almost completely metabolised under the used conditions with only the traces detected in 10% DMSO- d_6 /90% D_2O , and some 10% of picoplatin found in 1% DMSO- d_6 /99% D_2O after 24 h of standing at r.t. This observation also proved that the DMSO concentration is decisive for the rate and extent of the picoplatin degradation. Regarding the last set of experiments performed by ^1H NMR in PBS-buffered 10% DMSO- d_6 /90% PBS in D_2O (Figure S4) and in 1% DMSO- d_6 /99% PBS in D_2O (Figure S5), the results proved the release of α -picoline under the used experimental conditions. Specifically, the characteristic C6–H signal was detected at 8.26 ppm in both the PBS-buffered solution, which correlated well with free α -picoline. Again, higher extent of the picoplatin degradation was detected in 10% DMSO solution (<5% of picoplatin and *ca.* 20% of free picoline after 24 h of standing at r.t.) as compared with 1% DMSO solution (*ca.* 80% of picoplatin and *ca.* 5% of free picoline after 24 h of standing at r.t.).

The new signals detected in the ^1H NMR spectra of picoplatin in the used DMSO/water and DMSO/PBS (see Figures S2–S5), which do not belong to picoplatin or free pic, can be assigned to the DMSO-containing species, as proved by additional ESI-MS experiments. The obtained ESI $^+$ MS spectra showed a gradual increase of the relative intensity of the $\{[\text{Pt}(\text{DMSO})(\text{pic})]-\text{H}^+\}^+$ and $[\text{PtCl}(\text{DMSO})(\text{NH}_3)(\text{pic})]^+$ species (365.0 and 418.9 m/z , respectively) at the expense of picoplatin's signal at 398.9 m/z (the $\{[\text{PtCl}_2(\text{NH}_3)(\text{pic})]+\text{Na}^+\}^+$ species; Figure S6).

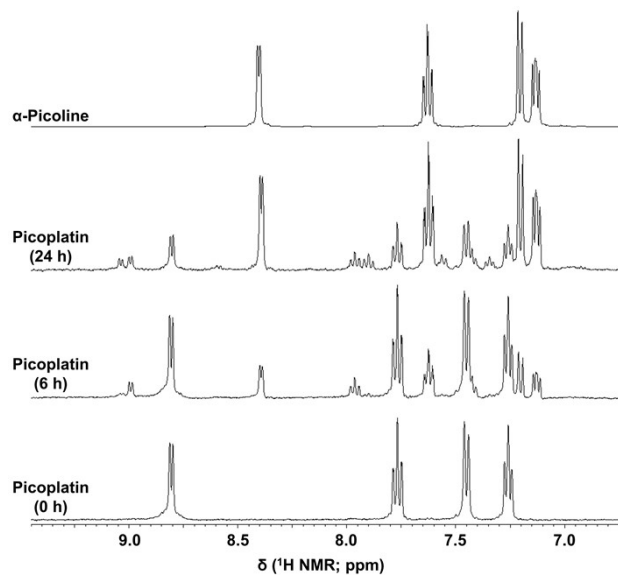


Figure S1. ^1H NMR spectra of picoplatin at different time points (0–24 h of standing at r.t.), given with free α -picoline. The studied compounds were dissolved in $\text{DMSO-}d_6$.

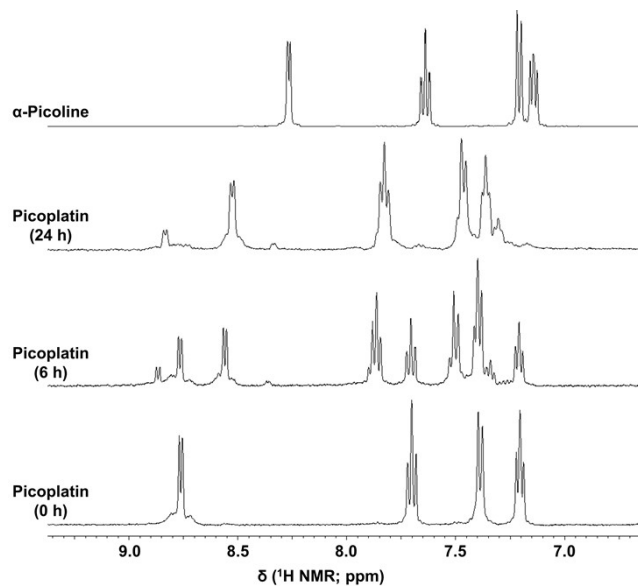


Figure S2. ¹H NMR spectra of picoplatin at different time points (0–24 h of standing at r.t.), given with free α -picoline. The studied compounds were dissolved in 10% DMSO-*d*₆/90% D₂O.

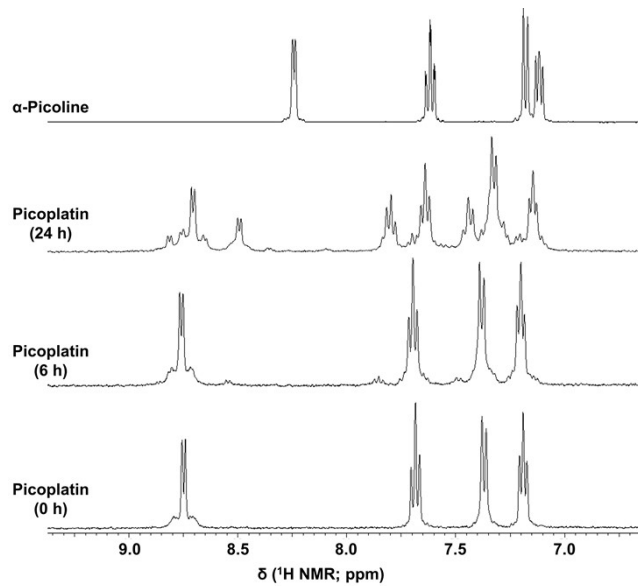


Figure S3. ¹H NMR spectra of picoplatin at different time points (0–24 h of standing at r.t.), given with free α -picoline. The studied compounds were dissolved in 1% DMSO-*d*₆/99% D₂O.

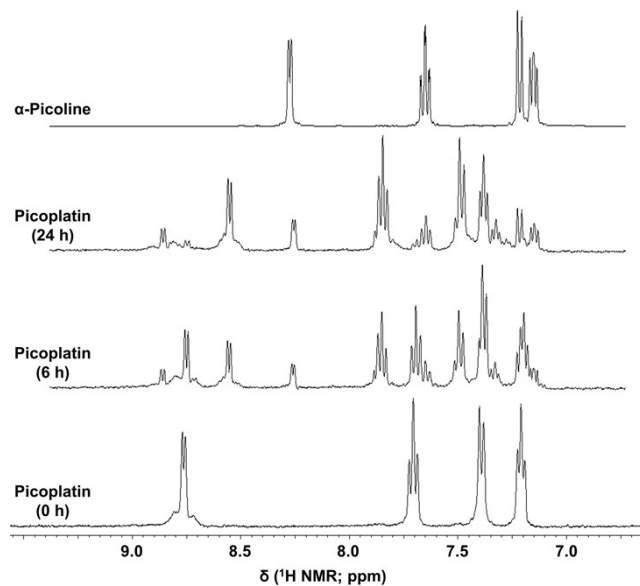


Figure S4. ¹H NMR spectra of picoplatin at different time points (0–24 h of standing at r.t.), given with free α -picoline. The studied compounds were dissolved in 10% DMSO-*d*₆/90% PBS in D₂O.

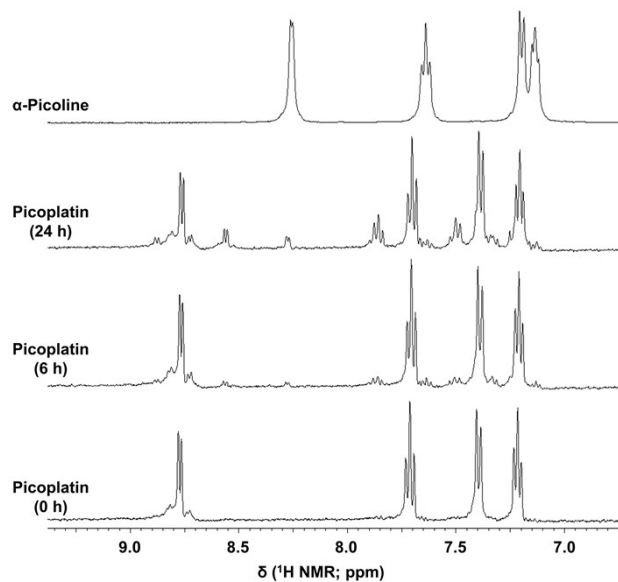


Figure S5. ¹H NMR spectra of picoplatin at different time points (0–24 h of standing at r.t.), given with free α -picoline. The studied compounds were dissolved in 1% DMSO-*d*₆/99% PBS in D₂O.

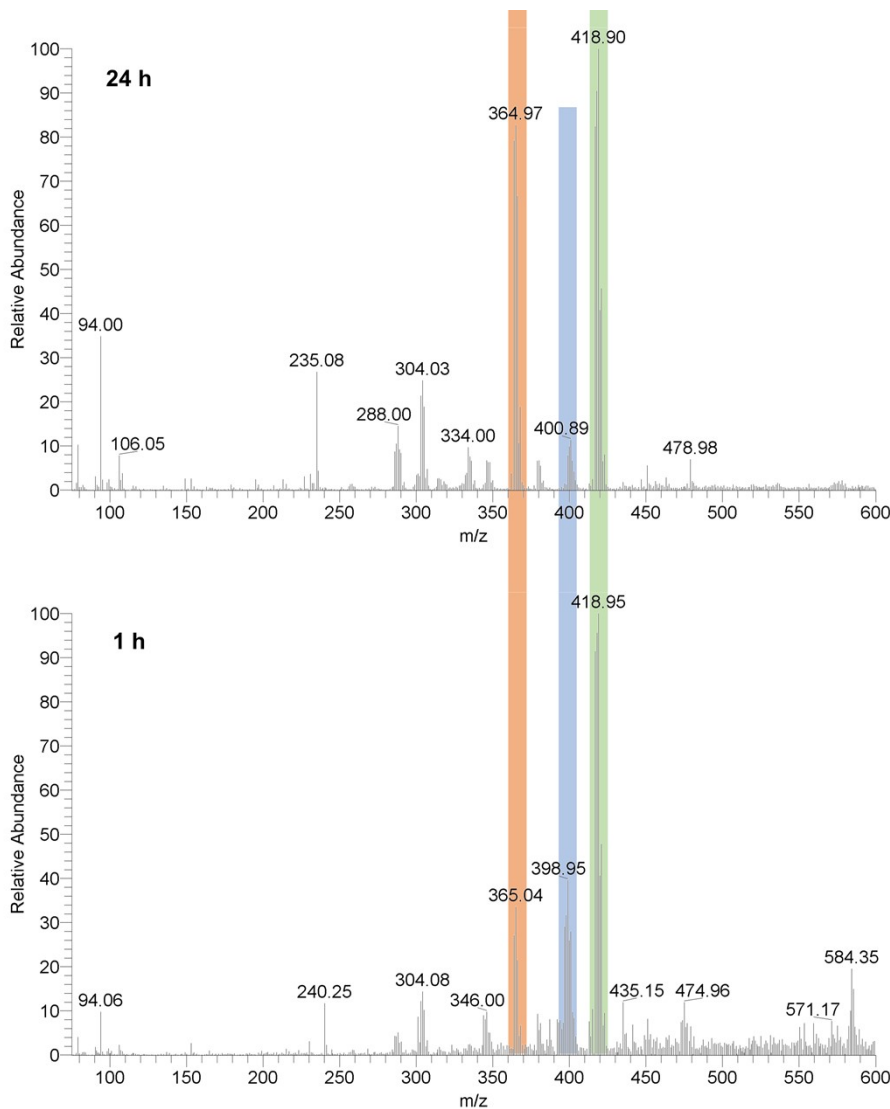


Figure S6. ESI+ mass spectrometry results for picoplatin dissolved in 1% DMSO-*d*₆/99% D₂O, as observed at different time points.

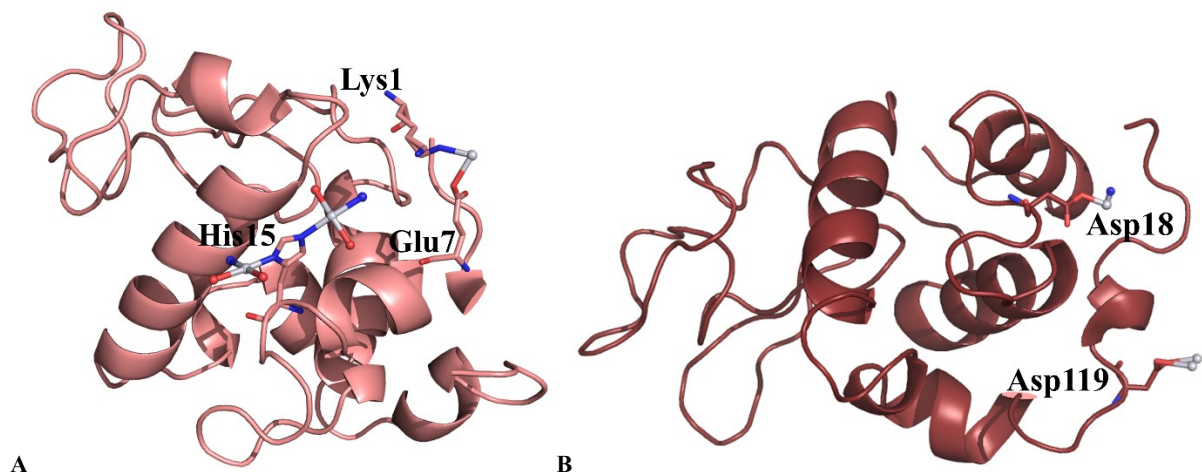
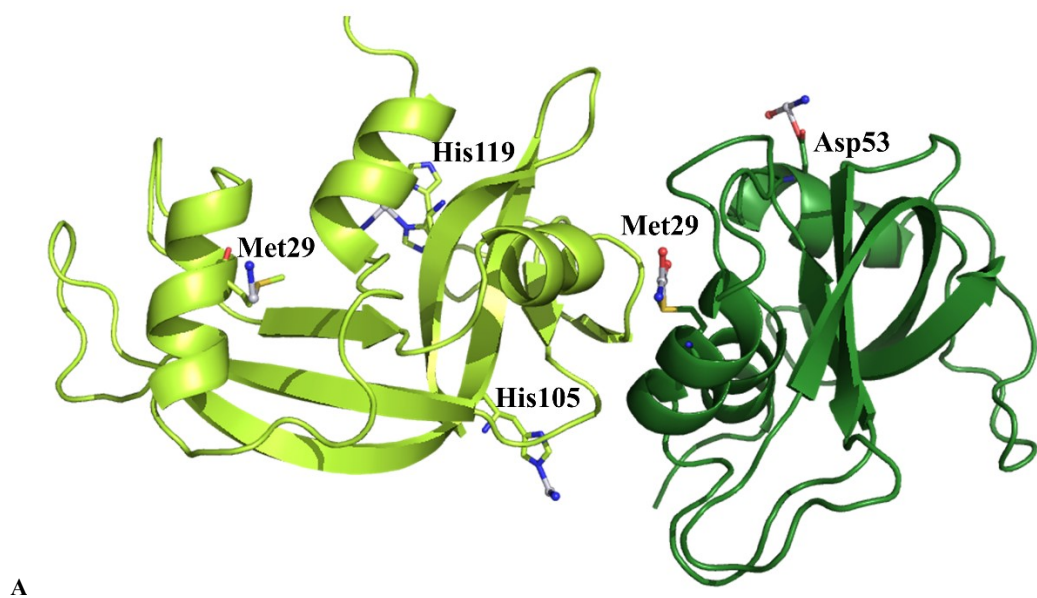


Figure S7. Overall structure of the adducts obtained upon reaction of HEWL with picoplatin under the two experimental conditions: structure **A** (panel A) and structure **B** (panel B). In both structures the platinum binding sites are shown.



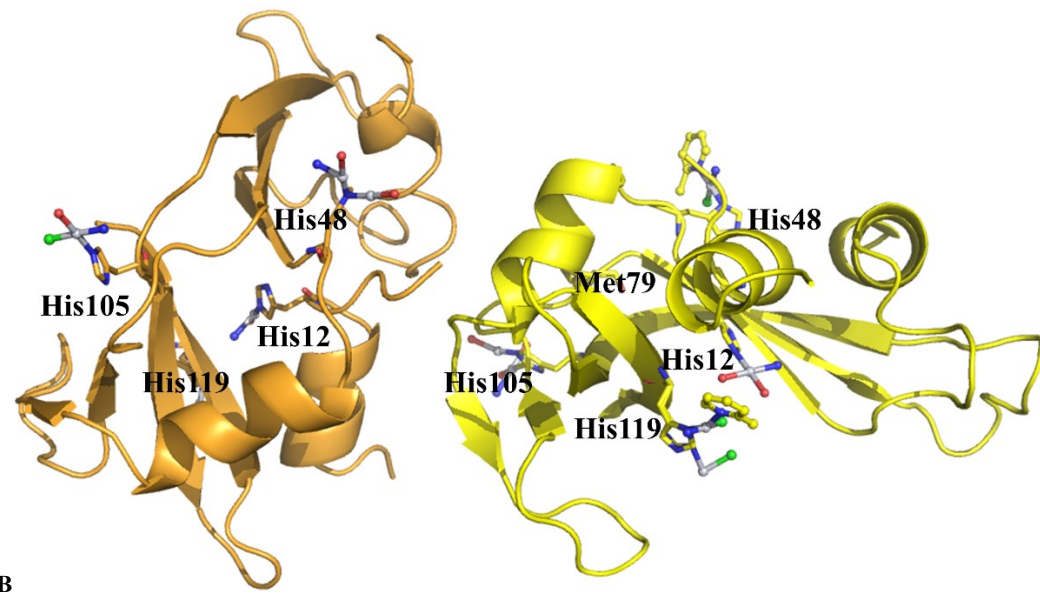


Figure S8. Overall structure of the adducts obtained upon reaction of RNase A with picoplatin under the two experimental conditions. Structure **C** is reported in panel A. Chain 1 is in forest green, chain 2 in lime green. Structure **D** is reported in panel B. Chain 1 is in bright orange, chain 2 is in yellow. In both structures the platinum binding sites are shown.

Table S1. The results of ESI⁺ mass spectrometry for picoplatin studied in various DMSO-containing solvents, as detected after 1h or 24 h of incubation.

Solvent (time point)	Species	Detected <i>m/z</i>	Calculated <i>m/z</i>	Relative intensity
DMSO (1 h)	$\{(pic)+H^+\}^+$ $\{[Pt(DMSO)(pic)]-H^+\}^+$ $\{[PtCl_2(NH_3)(pic)]+Na^+\}^+$ $[PtCl(DMSO)(NH_3)(pic)]^+$	94.0 365.0 398.9 418.9	94.1 365.0 399.0 419.0	20% 100% 55% 75%
DMSO (24 h)	$\{(pic)+H^+\}^+$ $\{[Pt(DMSO)(pic)]-H^+\}^+$ $[PtCl(DMSO)(NH_3)(pic)]^+$	94.0 365.0 418.9	94.1 365.0 419.0	20% 100% 90%
10% DMSO/90% H ₂ O (1 h)	$\{(pic)+H^+\}^+$ $\{[Pt(DMSO)(pic)]-H^+\}^+$ $[PtCl(DMSO)(NH_3)(pic)]^+$	94.0 365.0 418.9	94.1 365.0 419.0	20% 60% 100%
10% DMSO/90% H ₂ O (24 h)	$\{(pic)+H^+\}^+$ $\{[Pt(NH_3)(pic)]-H^+\}^+$ $\{[Pt(DMSO)(pic)]-H^+\}^+$ $\{[PtCl_2(NH_3)(pic)]+Na^+\}^+$ $[PtCl(DMSO)(NH_3)(pic)]^+$	94.0 304.1 365.0 398.9 418.9	94.1 304.0 365.0 399.0 419.0	30% 15% 100% 5% 65%
1% DMSO/99% H ₂ O (1 h)	$\{(pic)+H^+\}^+$ $\{[Pt(NH_3)(pic)]-H^+\}^+$ $\{[Pt(DMSO)(pic)]-H^+\}^+$ $\{[PtCl_2(NH_3)(pic)]+Na^+\}^+$ $[PtCl(DMSO)(NH_3)(pic)]^+$	94.1 304.1 365.0 399.0 419.0	94.1 304.0 365.0 399.0 419.0	10% 15% 35% 40% 100%
1% DMSO/99% H ₂ O (24 h)	$\{(pic)+H^+\}^+$ $\{[Pt(NH_3)(pic)]-H^+\}^+$ $\{[Pt(DMSO)(pic)]-H^+\}^+$ $[PtCl(DMSO)(NH_3)(pic)]^+$	94.0 304.0 365.0 418.9	94.1 304.0 365.0 419.0	35% 25% 85% 100%
10% DMSO/90% PBS in D ₂ O (1 h)	$\{(pic)+H^+\}^+$ $\{[Pt(DMSO)(pic)]-H^+\}^+$ $\{[PtCl_2(NH_3)(pic)]+Na^+\}^+$ $[PtCl(DMSO)(NH_3)(pic)]^+$	94.0 365.0 398.9 418.9	94.1 365.0 399.0 419.0	35% 100% 45% 20%
10% DMSO/90% PBS in D ₂ O (24 h)	$\{(pic)+H^+\}^+$ $\{[Pt(NH_3)(pic)]-H^+\}^+$ $\{[Pt(DMSO)(pic)]-H^+\}^+$ $\{[PtCl_2(NH_3)(pic)]+Na^+\}^+$ $[PtCl(DMSO)(NH_3)(pic)]^+$	94.0 304.0 365.0 398.9 418.9	94.1 304.0 365.0 399.0 419.0	40% 20% 100% 10% 15%
1% DMSO/99% PBS in D ₂ O (1 h)	$\{[PtCl_2(NH_3)(pic)]+Na^+\}^+$	398.9	399.0	45%
1% DMSO/99% PBS in D ₂ O (24 h)	$\{(pic)+H^+\}^+$ $\{[Pt(NH_3)(pic)]-H^+\}^+$ $\{[Pt(DMSO)(pic)]-H^+\}^+$ $\{[PtCl_2(NH_3)(pic)]+Na^+\}^+$ $[PtCl(DMSO)(NH_3)(pic)]^+$	94.0 304.0 365.0 398.9 418.9	94.1 304.0 365.0 399.0 419.0	50% 25% 100% 20% 15%

Table S2. Data collection and refinement statistics.

	<i>Structure A</i>	<i>Structure B</i>	<i>Structure C</i>	<i>Structure D</i>
Protein	<i>HEWL</i> <i>With DMSO</i>	<i>HEWL</i> <i>Without DMSO</i>	<i>RNase A</i> <i>With DMSO</i>	<i>RNase A</i> <i>Without DMSO</i>
PDB code	9ENZ	9EO2	9EO5	9EO8
Space group	P4 ₃ 2 ₁ 2	P4 ₃ 2 ₁ 2	C2	C2
a (Å)	78.40	77.57	32.69	32.88
b (Å)	78.40	77.57	100.75	100.92
c (Å)	37.15	37.64	73.54	74.00
β (°)	90.00	90.0	90.46	X
Resolution range (Å)	39.20-1.60 (1.63-1.60)	38.78-1.36 (1.38-1.36)	50.37-1.99 (2.08-1.99)	28.83-1.76 (1.81-1.76)
Observations	345076 (17890)	591395 (30742)	98354 (4933)	148868 (7154)
Unique reflections	15767 (762)	25229 (1253)	16745 (844)	24352 (1413)
Completeness (%)	99.6 (99.3)	100.0 (100.0)	99.8 (99.8)	98.3 (78.8)
Redundancy	21.9 (23.5)	23.4 (24.5)	5.9 (5.8)	6.2 (5.1)
†Rmerge (%)	0.070 (1.253)	0.080 (2.079)	0.161 (0.999)	0.097 (0.792)
Average I/σ(I)	25.3 (3.2)	21.3 (2.2)	7.3 (2.1)	10.00 (1.70)
CC _{1/2}	0.999 (0.887)	0.999 (0.782)	0.988 (0.638)	0.996 (0.792)
Anom. Completeness (%)	99.5 (98.7)	100.0 (100.0)	99.3 (98.2)	97.0 (68.8)
Anom. Multiplicity	11.9 (12.9)	12.6 (12.8)	3.1 (3.0)	3.2 (2.8)
Resolution range (Å)	39.23-1.60	38.78-1.36	50.37-1.99	28.83-1.76
N° reflection (working set)	998	23465	1058	1600
N° non-H atoms (refinement)	1165	1230	2464	2144
R-factor/R _{free}	0.185/0.230	0.174/0.208	0.193/0.243	0.199/0.235
r.m.s.d. bonds	0.010	0.012	0.009	0.009
r.m.s.d. angles (°)	1.699	1.877	1.536	1.605
Most favoured	96.52	94.50	90.09	93.97
Outliers	0	0	4	2

References

- 1 Starha, P.; Drahos, B.; Herchel, R. An unexpected in-solution instability of diiodido analogue of picoplatin complicates its biological characterization. *Dalton Trans.*, **2021**, *50*, 6071-6075. <https://doi.org/10.1039/d1dt00740h>.
- 2 Russo Krauss, I.; Ferraro, G.; Pica, A.; Marquez, J.A.; Helliwell, J.H.; Merlini, A. Principles and methods used to grow and optimize crystals of protein–metallodrug adducts, to determine metal binding sites and to assign metal ligands. *Metalloomics*, **2017**, *9*, 1534-1547. <https://doi.org/10.1039/c7mt00219j>
- 3 C. Vonrhein, C Flensburg, P. Keller, A. Sharff, O. Smart, W. Paciorek, T. Womack, G. Bricogne. Data processing and analysis with the autoPROC toolbox. *Acta Crystallogr. Sect D* **2011**, *67*, 293-302. <https://doi.org/>
- 4 A.J. McCoy, R.W. Grosse-Kunstleve, P.D. Adams, M.D. Winn, L.C. Storoni and R.J. Read. Phaser crystallographic software. *J. Appl. Crystallogr.* **2007**, *40*, 658-674. <https://doi.org/>
- 5 J. M.C. Vaney, S. Maignan, M. Ries-Kautt and A Ducruix. High-resolution structure (1.33 Å) of a HEW lysozyme tetragonal crystal grown in the APCF apparatus. Data and structural comparison with a crystal grown under microgravity from SpaceHab-01 mission. *Acta Crystallogr. Sect. D* **1996**, *52*, 505-517. <https://doi.org/>
- 6 L. Vitagliano, A. Merlini, A. Zagari, L. Mazzarella. Reversible Substrate-Induced Domain Motions in Ribonuclease A. *Proteins* **2002**, *46*, 97-104. <https://doi.org/>
- 7 G.N. Murshudov, A.A. Vagin, E.J. Dodson. Refinement of Macromolecular Structures by the Maximum-Likelihood Method. *Acta Crystallogr. Sect. D* **1997**, *53*, 240-255. <https://doi.org/>
- 8 P. Emsley, K. Cowtan. Coot: model-building tools for molecular graphics. *Acta Crystallogr. Sect. D* **2004**, *60*, 2126-2132. <https://doi.org/>